02

# Theoretical investigation of magnetic resonance spectra of frustrated pseudoperovskite manganites

© L.E. Gonchar[1,2]

[1] Ural State University of Railway Transport,
620034 Yekaterinburg, Russia
[2] Ural Federal University after the first President of Russia B.N. Yeltsin,
620002 Yekaterinburg, Russia

e-mail: l.e.gonchar@urfu.ru

*Received October 30, 2022*
*Revised January 09, 2023*
*Accepted March 28.03.2023*

The magnetic resonance spectra of frustrated manganite compounds $La_{1/3}Ca_{2/3}MnO_3$ and $BiMnO_3$ are calculated within the framework of orbitally dependent magnetic interactions model. The aim of the paper is an investigation of orbital structure influence and superexchange interactions' competition effects on ferromagnetic or antiferromagnetic resonance spectra of these compounds. The description of the features of the resonance lower branches' dependencies on the magnitude and direction of the magnetic field is proposed. It is shown that the main influence on the symmetry of dependencies is exerted by single-ion anisotropy of the $Mn^{3+}$ ion, associated not only with the orbital structure, but also with the tilting distortions of oxygen octahedra around the ions.

**Keywords:** Manganites, orbital structure, multi-sublattice magnets, antiferromagnetic resonance.

DOI: 10.61011/EOS.2023.04.56357.57-22

## Introduction

Pseudo-perovskite manganites $R_{1-x}A_xMnO_3$ ($R^{3+}$ — rare earth elements or bismuth ions, $A^{2+}$ — alkaline earth ions, $x$ — doping level) are known as compounds with a Jahn-Teller ion sublattice, in which there are interesting properties due to the relationship between the crystal structure and the magnetic subsystem through orbital and charge orderings [1]. Because of the cooperative Jahn–Teller effect in the $Mn^{3+}$ sublattice, the symmetry of these crystals is lower than cubic. This effect, combined with the ordering of charge carriers, leads to various types of orbital structures, which, in turn, form unusual magnetic structures, including low-dimensional and frustrated ones.

The variety of magnetic structures is quite large among dielectric manganites. For example, pure orthorhombic manganites contain both canted magnetic structures [2,3] and helical incommensurate structures [4,5], in which exchange interactions with the next-nearest neighbors are supposed to compete [4]. The magnetic excitation spectra of such compounds have been well studied [6–8], but the angular dependences of the spectra for the case of frustration have not been studied experimentally. In the series of manganites, there are also frustrated magnets with a hexagonal crystal structure, in which $Mn^{3+}$ is orbitally non-degenerate, and the competition of exchange interactions arises for geometric reasons [9,10].

$BiMnO_3$ is the only frustrated manganite from the $RMnO_3$ series that does not have an orthorhombic or hexagonal structure. The orbital structure of this monoclinic crystal causes exchange interaction competition between nearest neighbors [9,11]. Complex crystal and orbital structures lead to a fairly simple uniaxial ferromagnetic ordering [12]. Thus, it is impossible to study the orbital structure and characteristics of magnetic interactions only from the magnetic structure in this compound.

For charge-ordered (CO) phases of manganites, compounds with a fraction of nonisovalent impurity $x = 1/2$ are well studied. As a result of, additional charge carriers appear, which in CO phase can be localized on manganese ions. The checkerboard ordering of the $Mn^{3+}/Mn^{4+}$ ions leads to zigzag orbital and magnetic ordering. The magnetic $CE$ structure with an easy axis directed along the $c$ axis is quasi-one-dimensional, consisting of ferromagnetic zigzags coupled antiferromagnetically [13]. There is no competition between orbitally dependent superexchange interactions, at least for R = La, Pr and A = Ca [13,14]. For the case R = Bi, competition may arise [15] as a cause of the $CE'$-structure [16,17], but this assumption has not yet been experimentally confirmed. The spectra of low-dimensional half-doped compounds with the $CE$ structure were studied from the point of view of the dispersion [18] and field [14] dependences, due to which the parameters of the superexchange interaction were determined and the influence of the orbital structure on the field dependences was shown low-frequency part of the spectrum [15].

The charge-ordered phase of manganite with $x = 2/3$ is the so-called „Wigner crystal“ [19,20]. The alternation of $Mn^{3+}/Mn^{4+}$ ions according to the type of a Wigner crystal means that there are two lines of $Mn^{4+}$ ions per line of $Mn^{3+}$ ions. The lines are parallel to the $c$ axis and alternate along the $a$ axis. The orbital-charge structure of

this compound leads to competition between exchange interactions, resulting in the formation of a magnetic structure consisting of mutually perpendicular trimers [19–21].

Thus, frustration in $La_{1/3}Ca_{2/3}MnO_3$ and $BiMnO_3$ manganites does not arise due to geometric reasons, as in compounds with a triangular or hexagonal lattice [10,22], and not due to competition between interactions between nearest and next-nearest neighbors [4,5,22]. The reason for the emergence of competition in this case is associated exclusively with the difference in exchange interactions in different directions due to the orbital ordering on the ions $Mn^{3+}$ [11,21]. It is necessary to find out to what extent the orbital structure (in case of $BiMnO_3$) or the orbital-charge structure (in case of $La_{1/3}Ca_{2/3}MnO_3$), leading to competing exchange interactions, will change the magnetic resonance spectra of the magnetically ordered phase compared to the structures leading to no magnetic frustration. However, the effect of competing exchange interactions on resonance spectra has not been studied. The theoretical description of the influence of the orbital structure and competition of exchange interactions on the magnetic resonance spectra in $La_{1/3}Ca_{2/3}MnO_3$ and $BiMnO_3$ compounds is the aim of this paper.

## Model of superexchange interaction and single-ion anisotropy

The superexchange interaction depends on the orbital state of each interacting ion in the exchange pair. The orbital state $Mn^{3+}$ is described by the mixing angle $\Theta$ of the multielectron wave functions of the ground state [21]:

$$J_{ij}(\Theta_i, \Theta_j) = \frac{J_{0,k}\cos^2\varphi_{ij}}{r_{ij}^{10}} F_{ij}^k(\Theta_i, \Theta_j), \qquad (1)$$

where the configuration parameters of the interacting pair are $\varphi_{ij}$ (bond angle Mn–O–Mn) and $r_{ij}$ (average bond length Mn–O in the $i-j$ pair). Other parameters depend on the charge or orbital states of the interacting ions in a pair: the index $k$ enumerates the types of pairs for which the exchange interaction parameter $J_{0,k}$ is different, $F_{ij}^k(\Theta_i, \Theta_j)$ is an orbitally dependent function. Its dependence on the orbital mixing angles $\Theta_i$, $\Theta_j$, causing unusual magnetic structures, is of three types.

1. The pair $Mn^{3+}$–$Mn^{3+}$ $(k=1)$,

$$F_{z,ij}^1(\Theta_i, \Theta_j) = 1 - \alpha(\cos\Theta_i + \cos\Theta_j) + \beta\cos\Theta_i\cos\Theta_j,$$

$$F_{x(y),ij}^1(\Theta_i, \Theta_j) = 1 + \frac{\alpha}{2}(\cos\Theta_i \pm \sqrt{3}\sin\Theta_i + \cos\Theta_j \pm$$

$$\sqrt{3}\sin\Theta_j) + \frac{\beta}{4}(\cos\Theta_i \pm \sqrt{3}\sin\Theta_i)(\cos\Theta_j \pm \sqrt{3}\sin\Theta_j).$$

2. The pair $Mn^{3+}$–$Mn^{4+}$ $(k=2)$,

$$F_{z,ij}^2(\Theta_i) = 1 - \alpha'\cos\Theta_i,\ F_{x(y),ij}^2(\Theta_i)$$

$$= 1 + \frac{\alpha'}{2}(\cos\Theta_i \pm \sqrt{3}\sin\Theta_i).$$

3. The pair $Mn^{4+}$–$Mn^{4+}$ $(k=3)$ — the exchange interaction does not depend on the orbital state, therefore $F^3 \equiv 1$.

The parameters $J_{0,1} = 1.69 \cdot 10^4\,\mathrm{K}\cdot\text{Å}^{10}$, $J_{0,2} = -2.6 \cdot 10^4\,\mathrm{K}\cdot\text{Å}^{10}$, $J_{0,3} = 1.1 \cdot 10^4\,\mathrm{meV}\cdot\text{Å}^{10}$, $\alpha = 1.0$, $\beta = 4.5$, $\alpha' = 2.8$ are semiempirical [21].

The single-ion anisotropy for $Mn^{3+}$ in the $p$ sublattice in the local axes of the oxygen octahedron is given [21] by the relation

$$H_{an}^{(p)} = D_p S_{pz_l}^2 + E_p(S_{px_l}^2 - S_{py_l}^2), \qquad (2)$$

where $D_p = -3P\cos\Theta_p$, $E_p = -\sqrt{3}P\sin\Theta_p$, $P = -1.15\,\mathrm{K}$. $Mn^{4+}$ sublattices do not possess single-ion anisotropy.

## Magnetic structure and resonance spectra

The model of the magnetic subsystem [21] is the following:

$$\hat{H}_{mag} = \Sigma_{i>j} J_{ij}(\Theta_i, \Theta_j)(\mathbf{S}_i \cdot \mathbf{S}_j) +$$

$$\Sigma_{p,\alpha,\beta} D_p^{\alpha\beta}(\Theta_i) S_p^\alpha S_p^\beta + g\mu_B \Sigma_i(\mathbf{H}\cdot\mathbf{S}_i). \qquad (3)$$

The first term — the superexchange interaction, the parameters of which $J_{ij}(\Theta_i, \Theta_j)$ are calculated from the known experimental crystal, charge and orbital structures using the formula (1), the second one — the orbitally dependent single-ion anisotropy, determined by the formula (2) taking into account the transformation from the local to the general coordinate system (the summation goes only over the $Mn^{3+}$ ions), and the third one — the Zeeman interaction. The dependence of the $g$ tensor on the direction and orbital state of the $Mn^{3+}$ ions is ignored.

The sufficiency problem of the Hamiltonian contributions (3) requires special attention. On the one hand, it is traditional for manganites, especially for orthorhombic $RMnO_3$, to include the model of antisymmetric exchange interaction of Dzyaloshinskii–Moriya (DMI) . On the other hand, for pure $LaMnO_3$, it was shown that the inclusion of the DMI magnetic subsystem in the model in the form proposed in the experimental paper [25] does not change the qualitative characteristics of the angular and field dependence of the antiferromagnetic resonance spectra (AFMR) [27], because the crystal symmetry is taken into account in the single-ion anisotropy. Accounting for DMI is critical for EPR spectra, since it makes a essential contribution to the linewidth [24]. Meanwhile, the position of the line in the dependences of the AFMR spectrum with allowance for the DMI changes neglibly. For the compounds considered in this paper, there is an additional problem of taking into account the DMI, which is related to the lack of experimental data. The DMI vector parameter $\mathbf{d}_{ij} = d_{ij}[\mathbf{r}_i \times \mathbf{r}_j]$ between $i$ and $j$ ions, as shown in [28], is associated not only with the magnetic ion-ligand coupling vectors $\mathbf{r}_i$, $\mathbf{r}_j$, but also with the magnitude and sign of the $d_{ij}$ coefficient, additionally depending on the angle of

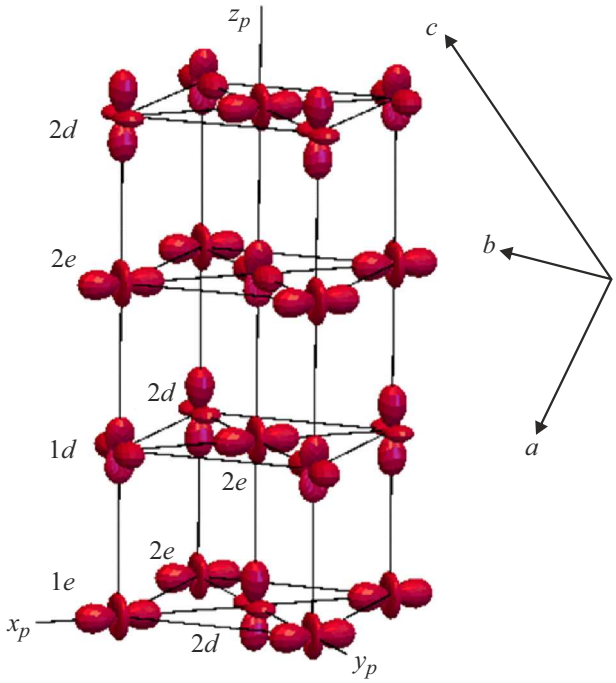


**Figure 1.** Orbital structure of $BiMnO_3$ in pseudo-perovskite axes ($x_p$, $y_p$, $z_p$), axes of the monoclinic coordinate system (*a, b, c*) are shown nearby. $Mn^{3+}$ ions are shown as electron densities, names of crystallographic positions are marked.

superexchange coupling. In addition, for Jahn-Teller (JT) compounds, the dependence of $d_{ij}$ on the orbital states of the interacting ions is also implied. Therefore, it is incorrect to use the experimental parameters of the papers [23–26] in this paper. The DMI simulation for $BiMnO_3$ was carried out in [29], however, only two possible directions of the $\mathbf{d}_{ij}$ vectors are given there, and only for the second neighbors. The DMI vectors for $Mn^{3+}-Mn^{4+}$ pairs, which are of decisive importance for $La_{1/3}Ca_{2/3}MnO_3$, are given in the review [22]. However, the coordination of the $Mn^{3+}$ ion in the paper [22] is non-octahedral, so the vectors cannot be used in the calculations of this paper. At present, studies of EPR spectra in doped manganites, including bismuth-containing and charge-ordered manganites, neglect this type of interaction [30]. The simulation of the spin wave and AFMR spectra for CO manganites with $x = 1/2$ also repeated the qualitative characteristics of the experimental dependences without taking into account the DMI [15]. The double exchange is not taken into account in the Hamiltonian (3), since the crystals are assumed to be dielectric, the charge carriers in the CO phase are assumed to be localized.

## $BiMnO_3$ compound

In $BiMnO_3$, which is a pseudoperovskite crystal, the crystal structure of the monoclinic system, described by the symmetry group $C2/c$, and the orbital ordering differ

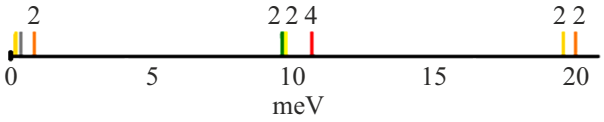


**Figure 2.** Model spectrum of magnetic excitations $BiMnO_3$. The numbers above indicate the number of spectrum branches in the given zone.

essentially from the orthorhombic manganites $RMnO_3$ [12]. The orbital ordering calculated in the linear vibronic model contradicts the ferromagnetic structure [11]. The competition of the superexchange parameters calculated without additional vibronic terms leads to an antiferromagnetic structure of the *C* type (ferromagnetic lines along the $x_p$ axis, antiferromagnetically ordered along other pseudoperovskite axes). $Mn^{3+}$ ions involved in the formation of the magnetic structure are divided into two positions, *d* and *e*, with different orbital states (Fig. 1). Taking into account the adjustments, the orbital ordering is given by the following expressions:

$$\Theta_{1e} = \Theta_{2e} = \Theta_e = 5\pi/3, \Theta_{1d} \approx 4\pi/3 - \Theta_{2d} = \Theta_d = \pi/2. \quad (4)$$

This orbital structure does not change the signs of the exchange parameters, but the equilibrium magnetic structure for competing exchange parameters becomes ferromagnetic [11]. Usually, to describe such a magnetic structure, one magnetic sublattice is sufficient, which describes the direction of the magnetic moment of any ion in the crystal. In this compound, it is important to use the model of 16 magnetic sublattices in order to take into account the difference in exchange interactions in pairs located in different directions of the crystal. The exchange interaction and single-ion anisotropy (in pseudoperovskite axes) are given in Table 1.

Accounting for the corrected orbital structure and tilting distortions of octahedra in single-ion anisotropy leads to an equilibrium ferromagnetic structure with easy magnetization along the *c* axis, which contradicts experimental studies [12], which determined the main direction of the magnetic structure along axes *b*. The reason for the contradictions is probably the demand to take into account a larger number of interactions or magnetic neighbors. Changes in the orbital structure were studied only from the point of view of a possible change in the angular characteristic of the orbital state of the *e* ($\Theta_e$) position, since the single-ion anisotropy of just this position stabilizes the direction along the *c* axis. However, no value of $\Theta_e$ results in experimental ordering. In this model, three slightly different directions of magnetization with a large total magnetic moment were obtained.

The simulation of the spectra of magnetic excitations of bismuth manganite was also carried out in the 16-sublattice model. Thus, there are 16 branches in the model spectrum (Fig. 2). Since there are only three different directions of magnetization, all 16 branches will not be

**Table 1.** Magnetic interactions in $BiMnO_3$ calculated with formulas (1), (2), (4); tilting distortions are not taken into account in anisotropy

| Ion $Mn^{3+}$ | Interaction with an ion | Exchange with the nearest neighbors, K | | | Ion $Mn^{3+}$ | Anisotropy, K | | |
|---|---|---|---|---|---|---|---|---|
| | | $J_x$ | $J_y$ | $J_z$ | | $D^{xx} = E$ | $D^{yy} = -E$ | $D^{zz} = D$ |
| 1*e* | 1*d* | -27.8 | -5.4 | 4.1 | 1*e* | -1.7 | 1.7 | 1.7 |
| | 2*d* | -27.8 | 4.1 | -5.4 | 2*e* | -1.7 | 1.7 | 1.7 |
| 2*e* | 1*d* | -27.8 | -5.4 | 4.1 | 1*d* | 2.0 | -2.0 | 0 |
| | 2*d* | -27.8 | 4.1 | -5.4 | 2*d* | 1.0 | -1.0 | -3.0 |

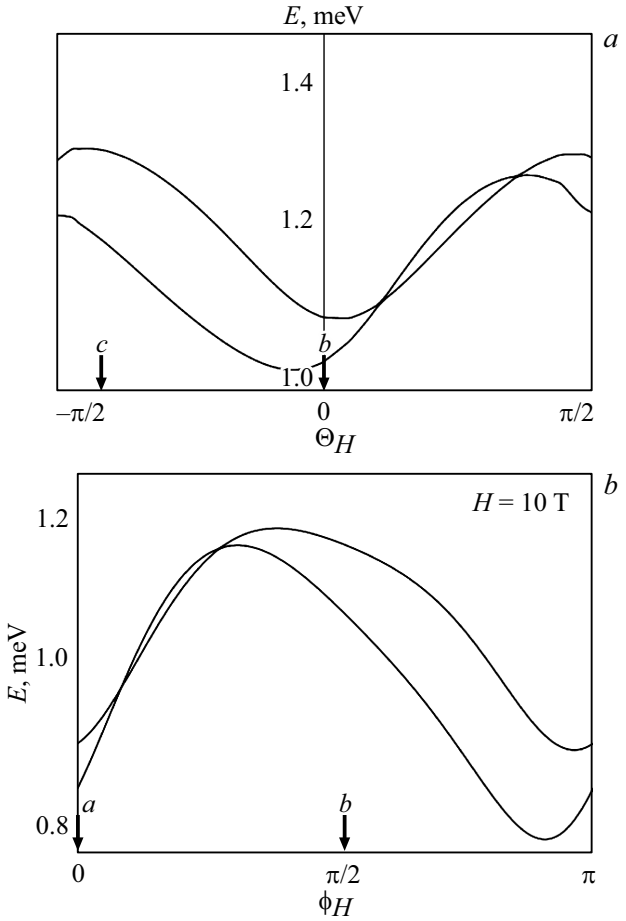


**Figure 3.** Angular dependences of ferromagnetic resonance energies in $BiMnO_3$ ($H = 10$ T): in the *bc* plane; (*b*) in the *ab* plane. The arrows and letters indicate the directions of the vectors of the lattice constants.

observed experimentally. It makes sense to review only the low-energy part of the spectrum. The gap in the spectrum is approximately 0.05 meV and is mainly proportional to the single-ion anisotropy constant $P$ .

The calculation of the field dependence of the spectrum does not give stable results in weak magnetic fields, especially since the shape of the sample and demagnetizing factors were not taken into account in the model (3). The angular dependence of the ferromagnetic resonance frequencies at sufficiently strong fields was calculated in order to isolate the contribution of the orbitally dependent single-ion anisotropy and note the effect of exchange competition (Fig. 3). Twofold symmetry is predicted on the dependences in the monoclinic planes *bc* and *ab*. The extrema of the dependences are shifted compared to the symmetric directions, which is due to the deviation of the model magnetization direction from the perpendicular to the *ab* plane. The influence of competition between exchange interactions and frustration of antiferromagnetic bonds in this dependence is expressed in the crossing of the dependences of two branches at asymmetric points. The angular dependence of the ferromagnetic resonance frequencies significantly differs from the dependence of the antiferromagnetic resonance frequencies in a compound with the similar formula $LaMnO_{33}$ [27], in which there is no competition between exchange interactions and the dependences of the lower branches do not cross. There are no experimental data on the study of the angular dependences of the magnetic resonance in the ordered phase in either compound.

## $La_{1/3}Ca_{2/3}MnO_3$ compound

$La_{1/3}Ca_{2/3}MnO_3$ is a charge-ordered (at low temperatures) orthorhombic manganite with symmetry group *Pnma* and alternation of $Mn^{3+}/Mn^{4+}$ ions in the magnetic and orbital subsystem [19] (Fig. 4). The orbital ordering of the $Mn^{3+}$ sublattice is given [21] by the relation

$$\Theta_1 = \Theta_4 = 2\pi - \Theta_2 = 2\pi - \Theta_3 \approx 5\pi/3. \qquad (5)$$

Exchange interactions for such an orbital structure compete, creating various types of ordering from strongly coupled ferromagnetic trimers $Mn^{4+}-Mn^{3+}-Mn^{4+}$, arranged in stripes parallel to the *c* axis (Fig. 5). The bonds between the $Mn^{4+}-Mn^{4+}$ ions in the *ac* plane are frustrated. At simulation of an equilibrium magnetic structure, it becomes essential to use 24 magnetic sublattices in order to take into account the difference in exchange interactions in pairs of different compositions and located in different directions. In this case, the magnetic cell doubles relative to the crystallographic one along the *c* axis and contains eight $Mn^{3+}$ ions and sixteen $Mn^{4+}$ ions. The exchange interaction

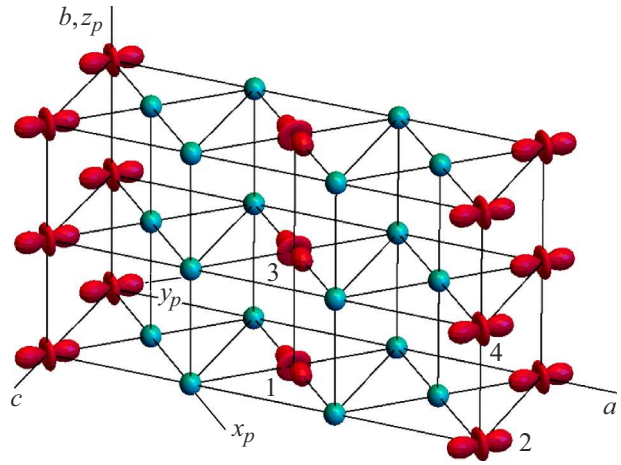


**Figure 4.** Charge-orbital structure of „Wigner crystal"-type $La_{1/3}Ca_{2/3}MnO_3$. $Mn^{3+}$ ions are shown as electron densities (red), $Mn^{4+}$ — as spheres (blue). The axes *a, b, c* — in the orthorhombic coordinate system, the $x_p$, $y_p$, $z_p$ axes — are pseudo-perovskite, the numbers denote the orbital sublattices $Mn^{3+}$.

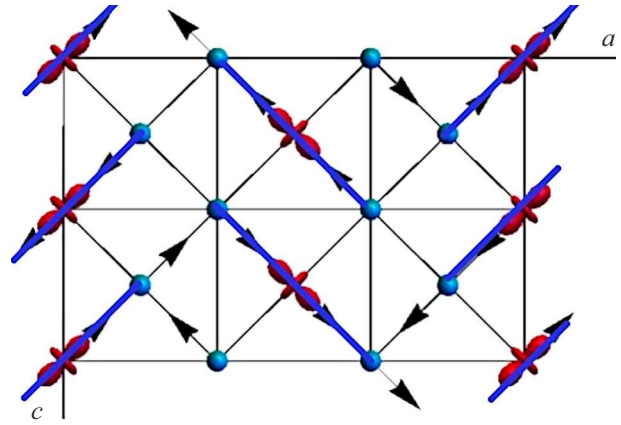


**Figure 5.** Perpendicular magnetic structure $La_{1/3}Ca_{2/3}MnO_3$ The direction of the magnetic moments in the neighboring (along the *b* axis) plane is opposite. Bold lines indicate strongly coupled magnetic trimers.

**Table 2.** Superexchange interactions in $La_{1/3}Ca_{2/3}MnO_3$ calculated by formulas (1), (5)

| Pair Type | Exchange Parameters, K |
|---|---|
| $Mn^{3+}-Mn^{3+}$ (*b*) | 30 |
| $Mn^{3+}-Mn^{4+}$ (*ac*) | 9 (between trimers), −117 (inside a trimer) |
| $Mn^{4+}-Mn^{4+}$ (*b*) | 15 |
| $Mn^{4+}-Mn^{4+}$ (*ac*) | 12 |

and single-ion anisotropy (in the pseudo-perovskite axes) are given in Tables 2, 3.

**Table 3.** Single-ion anisotropy parameters in $La_{1/3}Ca_{2/3}MnO_3$ on $Mn^{3+}$ sublattices , calculated by formulas (2), (5) without taking into account tilting distortions, in the local axes of the octahedron; ion numbers are given in accordance with orbital structure (5)

| Ion number $Mn^{3+}$ | Anisotropy, K | | |
|---|---|---|---|
| | $D^{xx} = E$ | $D^{yy} = -E$ | $D^{zz} = D$ |
| 1, 4 | 1.7 | −1.7 | 1.7 |
| 2, 3 | −1.7 | 1.7 | 1.7 |

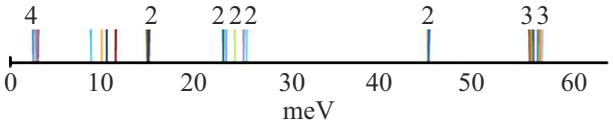


**Figure 6.** Model spectrum of magnetic excitations of $La_{1/3}Ca_{2/3}MnO_3$. The numbers above indicate the number of spectrum branches in the given zone.

Accounting for the orbital structure in expressions (1), (2) and tilting distortions of octahedra in single-ion anisotropy (2) leads to an equilibrium antiferromagnetic-perpendicular structure (Fig. 5) consisting of four different directions and eight magnetic sublattices (taking into account the difference between $Mn^{3+}$ and $Mn^{4+}$) [21]. Due to single-ion anisotropy in the equilibrium structure, the magnetic moment of each $Mn^{3+}$ ion is directed approximately along the elongated axis of the octahedron. The magnetic moments of $Mn^{4+}$, neighboring $Mn^{3+}$ in the direction of elongated bonds, are ordered in the same direction as $Mn^{3+}$ due to the strong ferromagnetic interaction, forming trimers. The perpendicular directions of the magnetic trimers are separated by antiferromagnetic stripes and directed along one of the pseudoperovskite axes $x_p$ or $y_p$ in each stripe. They are deviated from the axes (the angle between adjacent stripes is not 90°, but 80° or 110°) and has an small out-of-plane component. In this case, the total magnetization without an external magnetic field is equal to zero. The orbital structure $\Theta \approx 5\pi/3$ parameter is close to $1.73\pi$, at which the type of the magnetic structure changes [21]. Meanwhile, the magnetic structure itself can change its type from biaxial to canted uniaxial.

Calculation of the spectra of magnetic excitations was also carried out in the model of 24 magnetic sublattices. As a result of the calculations, 24 branches were obtained (Fig. 6). Since there are only eight sublattice with different directions and moduli of spins, eight branches should be observed in the spectrum, and the other branches will have zero intensity. In this connection, Fig. 7 shows only the low-energy part of the spectrum. The gap in the spectrum is approximately 2.8 meV. It is mainly proportional to $\sqrt{PJ_b}$ as in an antiferromagnet, coincides in order of magnitude with $LaMnO_3$

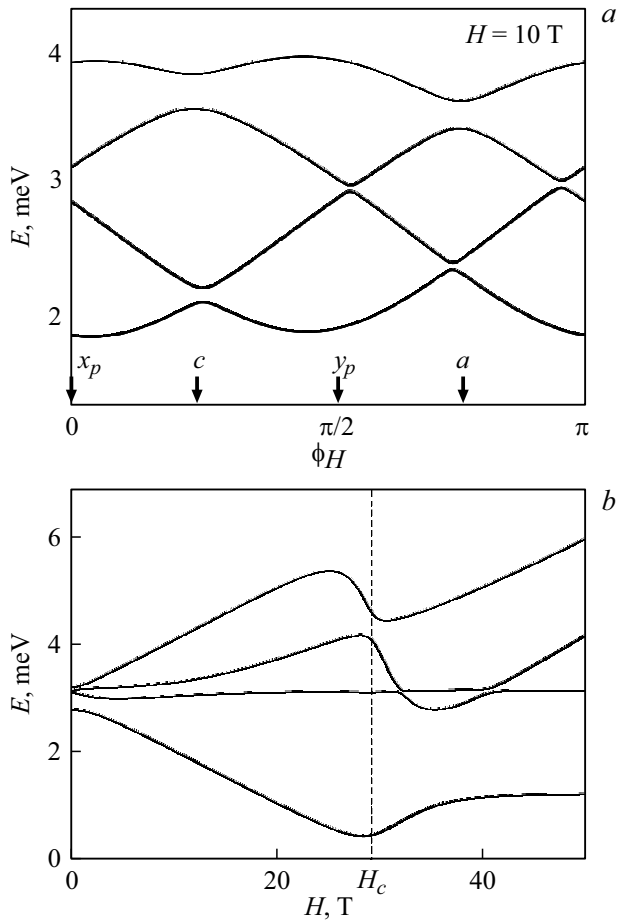


**Figure 7.** Dependences of the antiferromagnetic resonance energies in $La_{1/3}Ca_{2/3}MnO_3$ [15]: (*a*) on the direction of the external magnetic field in the $ac(x_py_p)$ plane, arrows and letters indicate the directions lattice constant vectors; (*b*) on the magnitude of the external magnetic field directed along one of the easy axes $x_p$ , $y_p$ in*ab* plane.

(2.7 meV [31,32]) and is larger than $Pr_{1/2}Ca_{1/2}MnO_{3-\delta}$ (0.64 meV [14]). Antiferromagnetic interactions in the *ac* plane are frustrated, and therefore have little effect on the gap.

The calculation of the dependence of the antiferromagnetic resonance spectrum on an external field directed along the pseudoperovskite axes $x_p$ or $y_p$ suggests the presence of features characteristic of a spin-flop transition [21]. Such a transition for this compound is possible for two directions of the external magnetic field, and spin „flopping“ occurs only in one of the stripes codirectional with the field. In this case, the stripe perpendicular to the field tends to the direction along the field. The value of the critical field — approximately 27 T. The field dependence is shown in Fig. 7,*a*. The spin-flop field mainly depends on the single-ion anisotropy and antiferromagnetic interactions and, to a lesser extent, on the ferromagnetic exchange parameter, despite its large value. The field corresponding to the spin-flop transition of codirectional stripes is presumably higher than in half-doped ($H_c \sim 6$ T [14]) and pure manganites ($H_c \sim 20$ T [31,32]) . This can be explained by the predominance of antiferromagnetic pairs with increasing impurity concentration. In this case, the average value of the single-ion anisotropy parameters for each manganese ion decreases, since the number of $Mn^{4+}$ ions without single-ion anisotropy increases in the cases of $x = 1/2$ and $x = 2/3$.

The dependence of the energy of low-frequency AFMR modes on the external magnetic field $La_{1/3}Ca_{2/3}MnO_3$ in two perpendicular directions of the *ac* plane is characteristic of a spin-flop transition (Fig. 7, *a*). Due to the increase in the number of sublattices, it is assumed that four modes (instead of two) will be observed in the low-energy part of the spectrum, as in a classical antiferromagnet [33], $LaMnO_3$ [7,32] or CO manganite at $x = 1/2$ [14,15].

The angular dependence of the AFMR spectrum (Fig. 7, *b*) is more affected by the orbital structure and the associated single-ion anisotropy. Despite two almost perpendicular easy axes, the angular dependence of the spectrum in the $ac(x_py_p)$ plane only approximately has a fourfold symmetry, differing in magnitude at the maxima and minima. This is due to accounting for tilting distortions of oxygen octahedra. The effect of the competition of exchange interactions is also expressed in the appearance of narrow gaps between the branches in the angular dependence of the spectrum.

## Conclusion

The magnetic resonance method in compounds with a complicated magnetic structure helps to refine its features indirectly. The angular dependence of the frequencies of the ferromagnetic (antiferromagnetic) resonance shows the symmetry of the magnetic subsystem. This dependence is mainly due to the equilibrium magnetic structure. The competition of exchange interactions has little effect on the shape of the angular dependences. However, for a frustrated compound, the atypical behavior of the dependences of the spectrum on an external magnetic field compared to easy-axis magnets is due to the nontrivial magnetic structure formed due to the competition of interactions. The angular dependence of the magnetic resonance spectra has a uniaxial type for $BiMnO_3$ and a biaxial type for $La_{1/3}Ca_{2/3}MnO_3$. For bismuth manganite, the calculations predict a magnetic easy axis that is stable to slight changes in the orbital structure and differs from the experiment [12]. The configuration of easy axes of lanthanum manganite with a high concentration of nonisovalent impurity, on the contrary, is sensitive to minor changes in the orbital structure, which was shown earlier [21].

### Conflict of interest

The author declares that she has no conflict of interest.

## References


[1] N.G. Bebenin, R.I. Zainullina, V.V. Ustinov. Physics-Uspekhi, **61**, 719(2018). DOI: D10.3367/UFNe.2017.07.038180.

[2] G. Matsumoto. J. Phys. Soc. Jap., **29**, 606 (1970). DOI: 10.1143/JPSJ.29.606

[3] Z. Jirák, S. Krupička, Z. Šimča, M. Dlouhá, S. Vratislav. J. Magn. Magn. Mater., **53**, 153 (1985). DOI: 10.1016/0304-8853(85)90144-1

[4] T. Kimura, S. Ishihara, H. Shintani, T. Arima, K.T. Takahashi, K. Ishizaka, Y. Tokura. Phys. Rev. B, **68**, 060403 (2003). DOI: 10.1103/PhysRevB.68.060403

[5] M. Mochizuki, N. Furukawa. Phys. Rev. B, **80**, 134416 (2009). DOI: 10.1103/PhysRevB.80.134416

[6] F. Moussa, M. Hennion, J. Rodriguez-Carvajal, H. Moudden, L. Pinsard, A. Revcolevschi. Phys. Rev. B, **54**, 15149 (1996). DOI: 10.1103/PhysRevB.54.15149

[7] K. Hirota, N. Kaneko, A. Nishizawa, Y. Endoh. J. Phys. Soc. Jap., **65**, 3736 (1996). DOI: 10.1143/JPSJ.65.3736

[8] Z. Chen, M. Schmidt, Z. Wang, F. Mayr, J. Deisenhofer, A.A. Mukhin, A.M. Balbashov, A. Loidl. Phys. Rev. B, **93**, 134406 (2016). DOI : 10.1103/PhysRevB.93.134406

[9] D.P. Kozlenko, S.E. Kichanov, S. Lee, J.-G. Park, V.P. Glazkov, B.N. Savenko. Crystallogr. Rep., **52**, 407 (2007). DOI: 10.1134/S1063774507030108

[10] S. Chattopadhyay, E. Ressouche, V. Simonet, V. Skumryev, A. Mukhin, V. Ivanov, M. Aroyo, D. Dimitrov. Phys. Rev. B, **98**, 134413 (2018). DOI: 10.1103/PhysRevB.98.134413

[11] L.E. Gonchar', A.E. Nikiforov. Phys. Rev. B, **88**, 094401 (2013). DOI: 10.1103/PhysRevB.88.094401

[12] D.P. Kozlenko, A.A. Belik, S.E. Kichanov, I. Mirebeau, D.V. Sheptyakov, T. Strässle, O.L. Makarova, A.V. Belushkin, B.N. Savenko. Phys. Rev. B, **82**, 014404(2010). DOI: 10.1103/PhysRevB.82.014404

[13] P.G. Radaelli, D.E. Cox, M. Marezio, S.-W. Cheong. Phys. Rev. B, **55**, 3015(1997). DOI: 10.1103/PhysRevB.55.3015

[14] S. Kawamata, S. Noguchi, K. Okuda, H. Nojiri, M. Motokawa. J. Magn. Magn. Mater., **226**–**230**, 854 (2001). DOI: 10.1016/S0304-8853(00)01290-7

[15] L.E. Gonchar'. Phys. Solid State, **61**, 728 (2019). DOI: 10.1134/S1063783419050093.

[16] C. Frontera, J.L. García-Muñoz, M.A. Aranda, C. Rittel, A. Llobet, M. Respaud, J. Vanacken. Phys. Rev. B, **64**, 054415 (2001). DOI: 10.1103/PhysRevB.64.054415

[17] A. Trokiner, S. Verkhovskii, A. Yakubovskii, K. Kumagai, S.-W. Cheong, D. Khomskii, Y. Furukawa, J.S. Ahn, A. Pogudin, V. Ogloblichev, A. Gerashenko, K. Mikhalev, Y. Piskunov. Phys. Rev. B, **72**, 054442 (2005). DOI: 10.1103/PhysRevB.72.054442

[18] R.A. Ewings, T.G. Perring, O. Sikora, D.L. Abernathy, Y. Tomioka, Y. Tokura. Phys. Rev. B, **94**, 014405 (2016). DOI: 10.1103/PhysRevB.94.014405

[19] P.G. Radaelli, D.E. Cox, L. Capogna, S.-W. Cheong, M. Marezio. Phys. Rev. B, **59**, 14440 (1999). DOI: 10.1103/PhysRevB.59.14440

[20] D.P. Kozlenko, L.S. Dubrovinsky, B.N. Savenko, V.I. Voronin, E.A. Kiselev, N.V. Proskurnina. Phys. Rev. B, **77**, 104444 (2008). DOI: 10.1103/PhysRevB.77.104444

[21] L.E. Gonchar'. J. Magn. Magn. Mater., **513**, 167248 (2020). DOI: 10.1016/j.jmmm.2020.167248

[22] S.-W. Cheong, M. Mostovoy. Nature Mater., **6**, 13 (2007). DOI: 10.1038/nmat1804

[23] I. Solovyev, N. Hamada, K. Terakura. Phys. Rev. Lett., **76**, 4825 (1996). DOI: 10.1103/PhysRevLett.76.4825

[24] D.L. Huber, G. Alejandro, A. Caneiro, M.T. Causa, F. Prado, M. Tovar, S.B. Oseroff. Phys. Rev. B, **61**, 12155 (1999). DOI: 10.1103/PhysRevB.61.12155

[25] D. Ivannikov, M. Biberacher, H.-A. Krug von Nidda, A. Pimenov, A. Loidl, A.A. Mukhin, A.M. Balbashov. Phys. Rev. B, **65**, 214422 (2002). DOI: 10.1103/PhysRevB.65.214422

[26] A. Mukhin, M. Biberacher, A. Pimenov, A. Loidl. J. Magn. Reson., **170**, 8 (2004). DOI: 10.1016/j.jmr.2004.05.019.

[27] A. Mozhegorov, L. Gontchar', A. Nikiforov. Appl. Magn. Reson., **33**, 167 (2008). DOI: 10.1007/s00723-008-0063-2

[28] A.S. Moskvin. JETP, 132, 517 (2021). DOI: 10.1134/S1063776121040245.

[29] I.V. Solovyev. Phys. Rev. B, **90**, 024417 (2014). DOI: 10.1103/PhysRevB.90.024417

[30] R. Singh, R. Ade. In: *Perovskite Materials*, London, ed. by Likun Pan, Guang Zhu (UK, IntechOpen Ltd., 2015), p. 331. DOI: 10.5772/61936

[31] L.E. Gonchar', A.E. Nikiforov, S.E. Popov. J. Exp. Theor. Phys., **91**, 1221 (2000). DOI: 10.1134/1.1342889.

[32] S. Mitsudo, K. Hirano, H. Nojiri, M. Motokawa, K. Hirota, A. Nishizawa, N. Kaneko, Y. Endoh. J. Magn. Magn. Mater., **177**–**181**, 877 (1998). DOI: 10.1016/S0304-8853(97)00525-8

[33] A.G. Gurevich, G.A. Melkov *Magnitniye kolebaniya i volny* (Nauka, M., 1994) (in Russian).


*Translated by E.Potapova*